Editors' Suggestion Featured in Physics

Physical Interpretation of Imaginary Time Delay

Isabella L. Giovannelli[*] and Steven M. Anlage
Maryland Quantum Materials Center, Department of Physics University of Maryland, College Park, Maryland 20742, USA

(Received 17 December 2024; revised 20 May 2025; accepted 3 June 2025; published 24 July 2025)

The scattering matrix S linearly relates the vector of incoming waves to outgoing wave excitations, and contains an enormous amount of information about the scattering system and its connections to the scattering channels. Time delay is one way to extract information from S, and the transmission time delay τ_T is a complex (even for Hermitian systems with unitary scattering matrices) measure of how long a wave excitation lingers before being transmitted. The real part of τ_T is a well-studied quantity, but the imaginary part of τ_T has not been systematically examined experimentally, and theoretical predictions for its behavior have not been tested. Here we experimentally test the predictions of Asano *et al.* [Nat. Commun. **7**, 13488 (2016)] for the imaginary part of transmission time delay in a nonunitary scattering system. We utilize Gaussian time-domain pulses scattering from a two-port microwave graph supporting a series of well-isolated absorptive modes to show that the carrier frequency of the pulses is changed in the scattering process by an amount in agreement with the imaginary part of the independently determined complex transmission time delay, $\mathrm{Im}[\tau_T]$, from frequency-domain measurements of the subunitary S matrix. Our results also generalize and extend those of Asano *et al.*, establishing a means to predict pulse propagation properties of non-Hermitian systems over a broad range of conditions.

DOI: 10.1103/nnk7-xy4v

Introduction—In linear scattering systems, the scattering matrix S is used to relate incoming waves $|\psi_{\mathrm{in}}\rangle$ to outgoing waves $|\psi_{\mathrm{out}}\rangle$ where $|\psi_{\mathrm{out}}\rangle = S|\psi_{\mathrm{in}}\rangle$. The scattering matrix S is a complex function of energy (or frequency) and is a square $M \times M$ matrix where M is the number of channels coupling the system to the outside world. This formulation of scattering as well as its statistical treatment using random matrix theory [1–9] can be applied to a wide array of complex systems. A nonexhaustive list includes microwave and sound scattering experiments [10–16], nuclear and atomic scattering [5], and scattering in quantum many-body systems [17]. The scattering matrix encapsulates a vast amount of information regarding the scattering system [5,18–20]. It can be used to determine how long a wave stays in the scattering system before leaving, which is referred to as time delay.

In the same way that the scattering matrix can be used to describe a broad range of scattering phenomena, time delay is just as widely applicable. In quantum mechanics, time delay is directly related to the phase evolution of quantum waves [21,22]. It can also be related to the density of states of open scattering systems [23,24]. In photonics, time delay can be used to determine group delay in optical fibers and manipulate the shape of wavefronts [25–29]. The time delay operator can also be utilized to optimize light storage within disordered media [30], and to characterize scattering of narrow-band acoustic pulses [31]. In electromagnetics, time delay can be used to determine group delay in wave guides [32–34] and to control the level of energy focused within a microwave enclosure [35]. It can also be used to determine the locations of poles and zeros of the scattering matrix in the complex frequency plane [7,36–40].

Time delay in unitary scattering systems—Time delay was first described by Eisenbud [41] and Wigner [42] in the context of elastic nuclear scattering. This concept was later generalized by Smith [43] to include inelastic scattering and systems with many channels. In the case of classical electromagnetic waves, the setting for the experimental results in this Letter, time delay is related to the derivative of the classical wave's scattering phase shift with respect to frequency [10,24,44]. Written in terms of the frequency dependent scattering matrix, the Wigner-Smith time delay for electromagnetic waves is $\tau_W(\omega) = -(i/M)[d/d\omega]\ln[\det S(\omega)]$ where ω is angular frequency.

The statistical properties of time delay in highly over-moded unitary scattering systems have been investigated in detail [7,45–58], including its use in quantum transport theory [59]. We note that furtive attempts to define a complex generalization of time delay in the context of tunneling [60,61] have proven to be of limited physical utility [62].

[*]Contact author: igiovann@umd.edu

Time delay in subunitary scattering systems—In this Letter, we will focus on the time delay associated with the transmission components of the scattering matrix referred to as transmission time delay (τ_T). This is in contrast to Wigner-Smith time delay which utilizes the entire scattering matrix. Since we study a two-port ring graph, the scattering matrix is rank 2: $S = \begin{pmatrix} R & T' \\ T & R' \end{pmatrix}$ where T and T' are the transmission coefficients and R and R' are the reflection coefficients. Transmission time delay $\tau_T = \tau_T(\omega; \alpha)$ is defined generally as [40]

$$\tau_T = -i \frac{\partial}{\partial \omega} \ln[\det T(\omega + i\alpha)] = \mathrm{Re}[\tau_T] + i\,\mathrm{Im}[\tau_T] \quad (1)$$

where $T = |S_{21}| e^{i\phi}$, and α quantifies the uniform loss in the system. Transmission time delay can be analogously defined for T'.

The transmission submatrix T is subunitary, hence τ_T is complex valued, and its real and imaginary parts can be either positive or negative. This naturally leads to the question of how to physically interpret this quantity.

Negative real time delay was examined theoretically by Garrett and McCumber [63] and experimentally demonstrated by Chu and Wong for light pulses interacting with a single isolated absorptive mode [64]. Negative time delay occurs when the group velocity (v_g) of the pulse surpasses the speed of light c, or becomes negative. This can occur in regions of large anomalous dispersion (e.g., the system is excited near one or more narrow resonances) [65]. In the $v_g > c$ case the peak of the pulse traveling through an anomalously dispersive medium arrives before an equivalent pulse traveling through vacuum [66]. In the $v_g < 0$ case the peak of the pulse leaves the medium before the peak of the incident pulse enters [67]. This unintuitive phenomenon is the result of inhomogeneous distortion of the Fourier components of the pulse as it travels through the medium, causing shifts in the center of the pulse and its leading edge. The overall pulse character is maintained as long as the frequency bandwidth of the pulse is smaller than the width of the resonance being excited in the medium [63,65]. Remarkably, a negative real part of complex time delay is also observed in media with gain [68], as well as loss, and in systems with nonlinear wave mixing [69]. Recently, in a purely quantum mechanical measurement of single photons traveling through a cloud of resonantly absorbing atoms a negative real part of time delay was observed [70], and its value is equal to the group delay [i.e., the real part of Eq. (1)], suggesting a deep connection between complex time delay and quantum weak measurements.

Imaginary time delay was first interpreted by Asano *et al.* [71] as a center-frequency shift in the pulse rather than a time shift. They note that this relationship is similar to that between frequency shifts and angular Goos-Hänchen shifts [72–76], as well as frequency shifts and the imaginary part of quantum weak measurement values [77–82]. Asano *et al.* make the theoretical connection between imaginary time delay and pulse center frequency shift but do not present corresponding experimental results. In this Letter, we extend their work by presenting the corresponding experimental results directly demonstrating the relationship between imaginary time delay and pulse center-frequency shift.

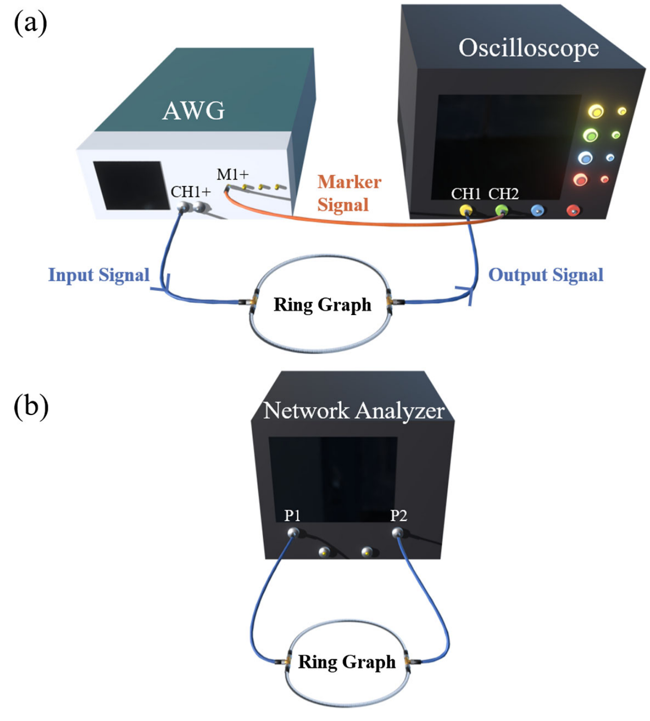

FIG. 1. (a) Time-domain experiment setup. (b) Frequency-domain experiment setup.

This Letter is structured as follows. First, we briefly review the theoretical model describing pulse propagation through dispersive media. We then present the experimental setup, data, and results. These experimental results are directly compared to the predictions made by Asano *et al.* [71], and we discuss how our results generalize theirs.

Transmission time delay and Gaussian pulse properties—To derive the predicted results one can combine methods used in Asano *et al.* [71] and Cao *et al.* [83]. The calculation details are presented in Sec. III of Supplemental Material [84]. Here we summarize the highlights. The main assumptions needed are: (1) The frequency bandwidth of the pulse $\tilde{\Delta}_\omega$ is much smaller than the 3-dB linewidth of the resonant mode being studied $\gamma_{3\text{-dB}}$, and (2) the system is linear and dispersive.

The predicted shift in transmission time (D_t) and center frequency (D_ω) of a transmitted Gaussian pulse is

$$D_t = \mathrm{Re}[\tau_T], \quad (2)$$

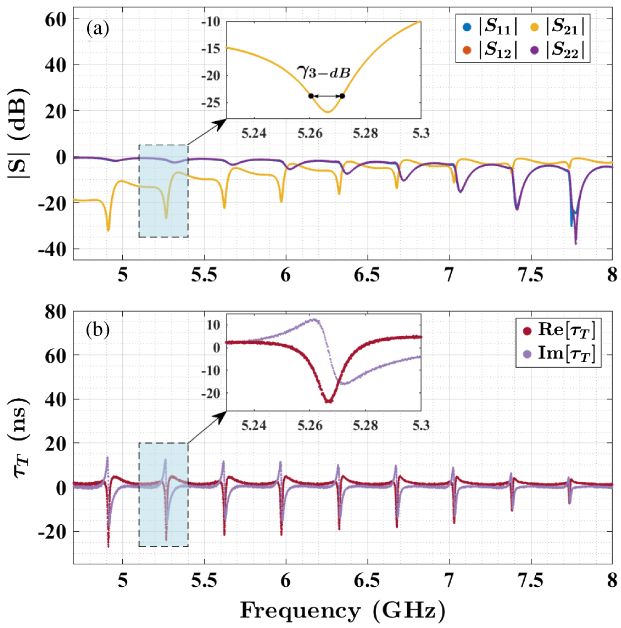

FIG. 2. (a) Measured scattering matrix elements for the ring graph depicted in Fig. 1(b). The transmission parameters are in orange and yellow (overlapping), the reflection parameters are in blue and purple. The inset is an enlarged graph of S_{21} for the indicated boxed region (5.23–5.3 GHz). The 3-dB bandwidth of this resonance is $\gamma_{3\text{-}dB} = 11.15$ MHz. (b) The transmission time delay is calculated using S_{21} data in (a). The real part is plotted in red and the imaginary part of the transmission time delay is plotted in light purple.

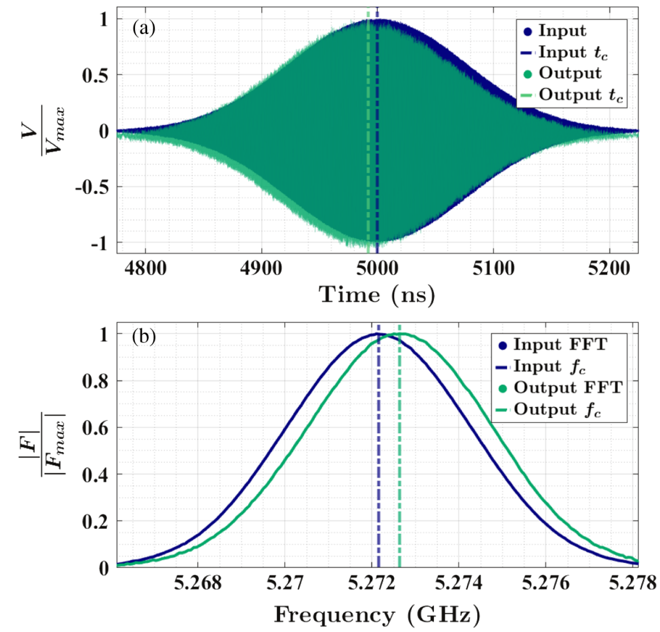

FIG. 3. (a) Example of normalized time domain data for the pulse transmission experiments. The dark blue trace is the pulse that is sent into the ring graph. This pulse has a center frequency of 5.2721 GHz and a frequency bandwidth of 5 MHz. The green trace is the output pulse from the ring graph. Their respective transmission times t_c are plotted as vertical dashed lines. (b) The Fourier transform of the time domain pulse data shown in (a), illustrating the center frequency shift.

$$D_\omega = -\tilde{\Delta}^2 \,\mathrm{Im}[\tau_T], \tag{3}$$

where $\tilde{\Delta} = (\tilde{\Delta}_\omega / 2\sqrt{2\ln 2})$ and $\tilde{\Delta}_\omega$ is the full width at half maximum (FWHM) of the pulse Gaussian distribution in the frequency domain. See Sec. V in Supplemental Material [84] for more details.

Experiment—The experiments were performed using a two-port microwave ring graph as the scattering system. The ring graph is composed of two coaxial cables of different lengths (27.9 and 30.5 cm long) and two T-junctions, and is depicted in both panels of Fig. 1. There are multiple reasons why we found it advantageous to use a ring graph for this experiment. One is that the ring graph has widely spaced and isolated absorptive modes [see Fig. 2(a)], allowing for straightforward analysis and interpretation. Another reason is because the S matrix and complex time delay of the ring graph have already been thoroughly characterized [40,85,86]. We note in passing that prior work has demonstrated that time delay of short pulses in microwave graphs contains useful information about the structure of the graph [87,88].

Transmission time delay measurements—To find the transmission time delay, we used the frequency domain experiment setup depicted in Fig. 1(b). Port 1 (P1) of a Keysight N5242A network analyzer (PNA-X) is attached to one end of the ring graph, the other end of the ring graph is attached to port 2 (P2). The PNA-X is calibrated up to the connection points to the ring graph with a Keysight N4691-60001 Electronic Calibration kit over the 10 MHz to 18 GHz frequency range with a frequency step size of 179.9 kHz.

Representative frequency domain results are summarized in Fig. 2, where both the measured scattering parameters and the corresponding calculated transmission time delay [using Eq. (1)] are depicted as a function of frequency. We see in Fig. 2(a) that the modes are widely spaced without any overlap as characterized experimentally in Ref. [40], and assumed theoretically [63,71].

In Fig. 2(b) we see that both the real and imaginary parts of the transmission time delay evolve through positive and negative values that can be described in terms of Lorentzian-based functions of frequency [39,40]. We also see that the transmission time delay extrema coincide with the scattering resonances.

Time domain Gaussian pulse measurements—The time domain measurements were performed using the setup depicted in Fig. 1(a). Channel 1 of a 50 GS/s Tektronix model AWG70001B arbitrary waveform generator (AWG) is attached to one end of the ring graph through a coaxial cable. The other end of the ring graph is attached, using another coaxial cable, to channel 1 of a Keysight Infiniium model UXR0104A 10-GHz bandwidth real-time digital sampling oscilloscope (DSO). The marker channel (M1+) of the AWG is attached to channel 2 of the DSO to trigger the oscilloscope and thus ensure measurements are all taken with the same zero time point. Please see Sec. V in Ref. [84] for details on how the Gaussian pulses were constructed and how the external delay from the cables was taken into account.

In Fig. 3(a) raw time domain data are shown for both the input and output pulses as well as the measured shifts in time and frequency. Note that the oscilloscope measures the detailed carrier-frequency oscillations of the pulse and not just its envelope. The input pulse shown here has a center frequency of 5.2721 GHz which situates it near the center of a resonance of the ring. The frequency bandwidth of the pulse is 5 MHz which is reasonably smaller than the 3-dB bandwidth of this resonance which is about 11.15 MHz. Since we are working in the small bandwidth limit, we calculate the transmission times (t_c) and center frequencies (ω_c) using the first temporal moment of the pulse [89,90], defined as

$$t_c = \frac{\int |V(t)|^2 t\, dt}{\int |V(t)|^2\, dt}, \tag{4}$$

$$\omega_c = \frac{\int |F(\omega)|^2 \omega\, d\omega}{\int |F(\omega)|^2\, d\omega}, \tag{5}$$

where V is the voltage, t is time, F is the magnitude of the Fourier transform of the time domain signal, and ω is angular frequency. The deduced transmission times and center frequencies are shown in Fig. 3 as vertical lines, demonstrating a negative real time delay of $D_t = -7.95$ ns and a positive center frequency shift of $D_\omega = 3.03$ Rad/μs or 0.00048 GHz.

Discussion—A full comparison of the Gaussian pulse measurements in the time domain with the predictions is summarized in Fig. 4. The data collected are over 4.9 GHz to 6.05 GHz, including four Feshbach modes, with 480 data points in total taken over the entire frequency range. [Also see Fig. 5 in Supplemental Material [84] for these results over a broader frequency range (10 MHz to 18 GHz), and Fig. 3 where we explore different pulse frequency bandwidths on a low transmission overlapping mode.]

We see from Fig. 4, that the measured center frequency shifts D_ω, as well as the measured time shift D_t, are in excellent agreement with the predictions of Asano *et al.* [Eqs. (2) and (3)] [71]. These results are also reproduced by simulations of the ring graph (see Sec. I of Ref. [84]). Note the difference in scales for the frequency shifts in Figs. 4(c) and 4(d), which shows that the frequency shift of the time-domain pulses increases with the predicted $\tilde{\Delta}^2$ scaling. Also note that Figs. 4(a) and 4(b) are nearly identical (i.e., independent of pulse bandwidth), as predicted. In all cases there are systematic deviations between the time-domain results and the predicted values from frequency-domain

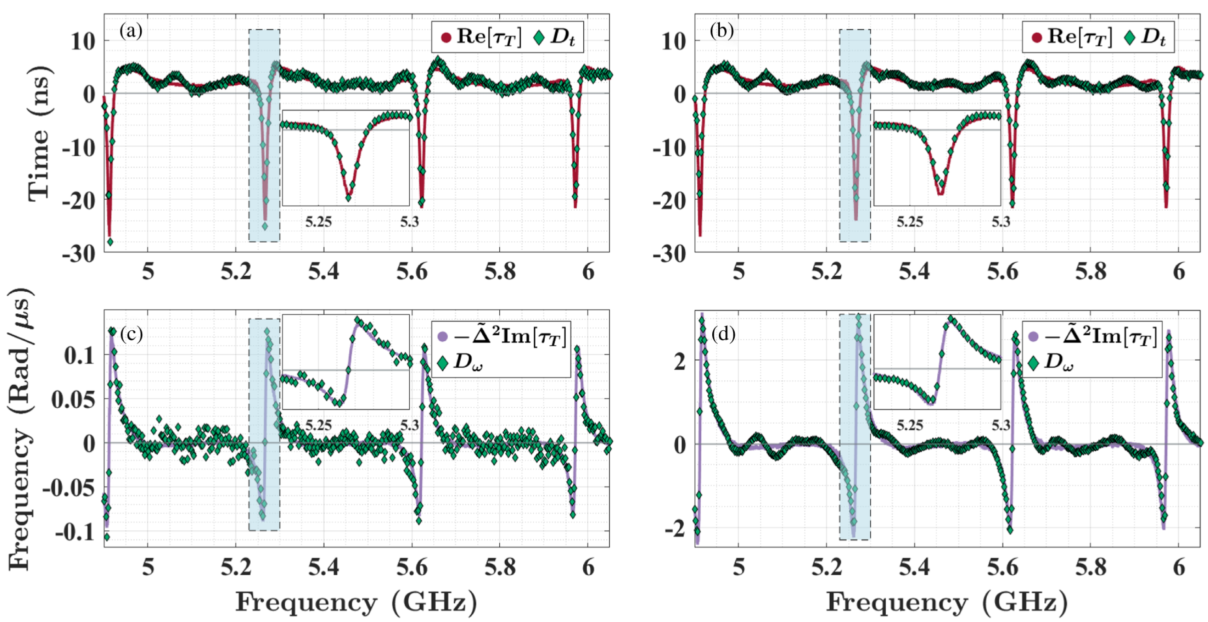

FIG. 4. Results for transmission time and center frequency shifts for an input pulse with a frequency bandwidth of 1 MHz [(a) and (c)] and 5 MHz [(b) and (d)]. In (a) and (b) the red curve corresponds to the right side of Eq. (2). Similarly in (c) and (d) the purple curve corresponds to the right side of Eq. (3). The green diamonds in plots in the top row (bottom row) are time domain experimental data where $D_t = t_c^{\text{output}} - t_c^{\text{input}}$ ($D_\omega = \omega_c^{\text{output}} - \omega_c^{\text{input}}$) is the difference in the calculated t_c (ω_c) between the input and the output pulses. These correspond to the left-hand side of Eqs. (2) and (3), respectively.

complex time delay in the range between the Feshbach modes. These deviations are attributed to standing waves on the input and output coaxial cables used in the time-domain measurements (see Ref. [84] Secs. I, II, and VI for more details).

One interesting observation is that the imaginary part of complex time delay produces changes in the carrier frequency so as to decrease the amount of absorption of the transmitted pulse [63,90]. Related to this, Ref. [91] shows a clear deviation from exponential decrease of laser intensity with propagation distance in a dispersive absorbing medium, showing that the light is less attenuated at greater distances than one would expect. In the case of a scattering system with gain, it has also been noted that the center frequency shift will be towards (rather than away from) the gain mode [63,90]. It is also worth pointing out that there is a clear correspondence between where negative time delay occurs and where the pulse center-frequency shifts are present. The physical mechanism behind these frequency shifts is the same as that giving rise to negative time delays, where they are a result of nonuniform distortion of the Fourier components of the pulse as it travels through a dispersive medium [63,65,67].

Asano *et al.* also make predictions for the maximum time and frequency shifts that can be created by a given scattering system in the critical coupling limit. These upper bounds are analogous to those for expectation values in quantum weak measurements, [71] and super-oscillatory functions [92,93]. The bounds on time and frequency shifts are given by $D_{t,\max} = \pm(1/\sqrt{2}\tilde{\Delta})$ and $D_{\omega,\max} = \pm(\tilde{\Delta}/\sqrt{2})$, respectively. In our case, for the pulses with a 1 MHz bandwidth, this would result in $D_{t,\max} \approx 265$ ns and $D_{\omega,\max} \approx 12$ Rad/μs, while for the 5 MHz bandwidth pulse case one has $D_{t,\max} \approx 53$ ns and $D_{\omega,\max} \approx 59$ Rad/μs. Our data for both of these cases, presented in Fig. 4 (as well as Fig. 5 in Sec. IV of Ref. [84]), are clearly well within these bounds, which is expected because the graph measurement is in the strong-coupling limit.

Our Letter generalizes that of Asano *et al.* [71] in the sense that our results for D_t and D_ω are not tied to any particular model of transmission near a resonant mode. We have shown instead that complex time delay derived from frequency-domain data provides model-free predictions for the pulse modifications due to scattering. We have shown that this includes frequencies that are far from resonant modes, where the analytical approximations are no longer valid.

Conclusions—In this Letter we experimentally demonstrate the connection between complex transmission time delay and Gaussian pulse properties; verifying the predictions first laid out in Ref. [71]. The most novel contribution is the direct connection between the imaginary component of the transmission time delay and the center frequency shift of the scattered Gaussian pulse. This helps bring physical meaning to an abstract but practically useful quantity that makes up the complex time delay.

This Letter establishes the detailed equivalence of complex scattering information derived from frequency-domain and time-domain approaches, providing insights that inform and simplify measurements over the entire electromagnetic spectrum.

In terms of future work, it would be interesting to generalize these predictions to arbitrary pulse shapes. It would also be interesting to see how this relation would hold for more complex scattering systems with overlapping modes, as well as for gain modes, or systems with strong nonlinearities. Additionally, we can now make predictions for reflection time delays, along with reflection time-delay differences [37,38], as well as transmission time-delay differences in nonreciprocal scattering systems [94]. The connection of this Letter to extreme time delays associated with scattering singularities [94,95] is also of interest.

Acknowledgments—We thank Nadav Shaibe for helpful discussions. This work was supported by NSF/RINGS under Grant No. ECCS-2148318, ONR under Grant No. N000142312507, and DARPA/WARDEN under Grant No. HR00112120021 and ONR/DURIP FY'25 under Grant No. N000142512140.

Data availability—The data that support the findings of this Letter are openly available [96].

[1] J. Verbaarschot, H. Weidenmüller, and M. Zirnbauer, Grassmann integration in stochastic quantum physics: The case of compound-nucleus scattering, Phys. Rep. **129**, 367 (1985).

[2] V. V. Sokolov and V. Zelevinsky, Dynamics and statistics of unstable quantum states, Nucl. Phys. **A504**, 562 (1989).

[3] H. Schomerus, Random matrix approaches to open quantum systems, in *Stochastic Processes and Random Matrices*, Lecture Notes of the Les Houches Summer School 2015, edited by G. Schehr, A. Altland, Y. V. Fyodorov, N. O'Connell, and L. F. Cugliandolo (Oxford University Press, New York, 2017), pp. 409–473.

[4] A. Nock, S. Kumar, H. J. Sommers, and T. Guhr, Distributions of off-diagonal scattering matrix elements: Exact results, Ann. Phys. (Amsterdam) **342**, 103 (2014).

[5] G. E. Mitchell, A. Richter, and H. A. Weidenmüller, Random matrices and chaos in nuclear physics: Nuclear reactions, Rev. Mod. Phys. **82**, 2845 (2010).

[6] P. A. Mello, P. Pereyra, and T. H. Seligman, Information theory and statistical nuclear reactions. I. General theory and applications to few-channel problems, Ann. Phys. (N.Y.) **161**, 254 (1985).

[7] Y. V. Fyodorov and H.-J. Sommers, Statistics of resonance poles, phase shifts and time delays in quantum chaotic scattering: Random matrix approach for systems with broken time-reversal invariance, J. Math. Phys. (N.Y.) **38**, 1918 (1997).

[8] Y. V. Fyodorov, D. V. Savin, and H.-J. Sommers, Scattering, reflection and impedance of waves in chaotic and disordered systems with absorption, J. Phys. A **38**, 10731 (2005).

[9] Y. Fyodorov and D. Savin, Resonance scattering of waves in chaotic systems, in *The Oxford Handbook of Random Matrix Theory* (Oxford University Press, New York, 2015).

[10] E. Doron, U. Smilansky, and A. Frenkel, Experimental demonstration of chaotic scattering of microwaves, Phys. Rev. Lett. **65**, 3072 (1990).

[11] A. Richter, Wave dynamical chaos: An experimental approach in billiards, Phys. Scr. **2001**, 212 (2001).

[12] U. Kuhl, O. Legrand, and F. Mortessagne, Microwave experiments using open chaotic cavities in the realm of the effective Hamiltonian formalism, Fortschr. Phys. **61**, 404 (2013).

[13] O. Hul, M. Ławniczak, S. Bauch, A. Sawicki, M. Kuś, and L. Sirko, Are scattering properties of graphs uniquely connected to their shapes?, Phys. Rev. Lett. **109**, 040402 (2012).

[14] G. Gradoni, J.-H. Yeh, B. Xiao, T. M. Antonsen, S. M. Anlage, and E. Ott, Predicting the statistics of wave transport through chaotic cavities by the random coupling model: A review and recent progress, Wave Motion **51**, 606 (2014).

[15] B. Dietz and A. Richter, Quantum and wave dynamical chaos in superconducting microwave billiards, Chaos **25**, 097601 (2015).

[16] U. Kuhl, H.-J. Stöckmann, and R. Weaver, Classical wave experiments on chaotic scattering, J. Phys. A **38**, 10433 (2005).

[17] A. Bereczuk, B. Dietz, J. Che, J. Kuipers, J.-D. Urbina, and K. Richter, Universal S -matrix correlations for complex scattering of wave packets in noninteracting many-body systems: Theory, simulation, and experiment, Phys. Rev. E **103**, 052209 (2021).

[18] D. Agassi, H. A. Weidenmüller, and G. Mantzouranis, The statistical theory of nuclear reactions for strongly overlapping resonances as a theory of transport phenomena, Phys. Rep. **22**, 145 (1975).

[19] L. Gao, L. Sun, F. Li, Q. Zhang, Y. Wang, T. Yu, J. Guo, Y. Bian, C. Li, X. Zhang, H. Li, J. Meng, and Y. He, 8-GHz narrowband high-temperature superconducting filter with high selectivity and flat group delay, IEEE Trans. Microwave Theory Tech. **57**, 1767 (2009).

[20] H. A. Weidenmüller, Stochastic scattering theory random-matrix models for fluctuations in microscopic and mesoscopic systems, in *Chaos and Quantum Chaos*, edited by W. D. Heiss (Springer, New York, 1992), pp. 121–166.

[21] D. Trabert, S. Brennecke, K. Fehre, N. Anders, A. Geyer, S. Grundmann, M. S. Schöffler, L. P. H. Schmidt, T. Jahnke, R. Dörner, M. Kunitski, and S. Eckart, Angular dependence of the Wigner time delay upon tunnel ionization of H_2, Nat. Commun. **12**, 1697 (2021).

[22] C.-H. Zhang and U. Thumm, Streaking and Wigner time delays in photoemission from atoms and surfaces, Phys. Rev. A **84**, 033401 (2011).

[23] J. Kuipers, D. V. Savin, and M. Sieber, Efficient semiclassical approach for time delays, New J. Phys. **16**, 123018 (2014).

[24] M. Davy, Z. Shi, J. Wang, X. Cheng, and A. Z. Genack, Transmission eigenchannels and the densities of states of random media, Phys. Rev. Lett. **114**, 033901 (2015).

[25] J. Carpenter, B. J. Eggleton, and J. Schröder, Observation of Eisenbud–Wigner–Smith states as principal modes in multimode fibre, Nat. Photonics **9**, 751 (2015).

[26] W. Xiong, P. Ambichl, Y. Bromberg, B. Redding, S. Rotter, and H. Cao, Spatiotemporal control of light transmission through a multimode fiber with strong mode coupling, Phys. Rev. Lett. **117**, 053901 (2016).

[27] J. Böhm, A. Brandstötter, P. Ambichl, S. Rotter, and U. Kuhl, In situ realization of particlelike scattering states in a microwave cavity, Phys. Rev. A **97**, 021801(R) (2018).

[28] B. Gérardin, J. Laurent, P. Ambichl, C. Prada, S. Rotter, and A. Aubry, Particlelike wave packets in complex scattering systems, Phys. Rev. B **94**, 014209 (2016).

[29] A. Brandstötter, A. Girschik, P. Ambichl, and S. Rotter, Shaping the branched flow of light through disordered media, Proc. Natl. Acad. Sci. U.S.A. **116**, 13260 (2019).

[30] M. Durand, S. M. Popoff, R. Carminati, and A. Goetschy, Optimizing light storage in scattering media with the dwell-time operator, Phys. Rev. Lett. **123**, 243901 (2019).

[31] U. R. Patel, Y. Mao, and E. Michielssen, Wigner–Smith time delay matrix for acoustic scattering: Theory and phenomenology, J. Acoust. Soc. Am. **153**, 2769 (2023).

[32] S. Fan and J. M. Kahn, Principal modes in multimode waveguides, Opt. Lett. **30**, 135 (2005).

[33] U. R. Patel and E. Michielssen, Wigner–Smith time-delay matrix for electromagnetics: Theory and phenomenology, IEEE Trans. Antennas Propag. **69**, 902 (2021).

[34] Y. Mao, U. R. Patel, and E. Michielssen, Wigner–Smith time delay matrix for electromagnetics: Systems with material dispersion and losses, IEEE Trans. Antennas Propag. **71**, 5266 (2023).

[35] P. Ambichl, A. Brandstötter, J. Böhm, M. Kühmayer, U. Kuhl, and S. Rotter, Focusing inside Disordered media with the generalized Wigner-Smith operator, Phys. Rev. Lett. **119**, 033903 (2017).

[36] Y. V. Fyodorov, S. Suwunnarat, and T. Kottos, Distribution of zeros of the S-matrix of chaotic cavities with localized losses and coherent perfect absorption: Non-perturbative results, J. Phys. A **50**, 30LT01 (2017).

[37] Y. Fyodorov, Reflection time difference as a probe of S-matrix zeroes in chaotic resonance scattering, Acta Phys. Pol. A **136**, 785 (2019).

[38] M. Osman and Y. V. Fyodorov, Chaotic scattering with localized losses: S-matrix zeros and reflection time difference for systems with broken time-reversal invariance, Phys. Rev. E **102**, 012202 (2020).

[39] L. Chen, S. M. Anlage, and Y. V. Fyodorov, Generalization of Wigner time delay to subunitary scattering systems, Phys. Rev. E **103**, L050203 (2021).

[40] L. Chen and S. M. Anlage, Use of transmission and reflection complex time delays to reveal scattering matrix poles and zeros: Example of the ring graph, Phys. Rev. E **105**, 054210 (2022).

[41] L. Eisenbud, The formal properties of nuclear collisions, Ph.D. thesis, Princeton University, 1948.

[42] E. P. Wigner, Lower limit for the energy derivative of the scattering phase shift, Phys. Rev. **98**, 145 (1955).

[43] F. T. Smith, Lifetime matrix in collision theory, Phys. Rev. **118**, 349 (1960).

[44] Y. Huang, Y. Kang, and A. Z. Genack, Wave excitation and dynamics in non-Hermitian disordered systems, Phys. Rev. Res. **4**, 013102 (2022).

[45] N. Lehmann, D. V. Savin, V. V. Sokolov, and H. J. Sommers, Time delay correlations in chaotic scattering: Random matrix approach, Physica (Amsterdam) **86D**, 572 (1995).

[46] V. A. Gopar, P. A. Mello, and M. Büttiker, Mesoscopic capacitors: A statistical analysis, Phys. Rev. Lett. **77**, 3005 (1996).

[47] T. S. Misirpashaev, P. W. Brouwer, and C. W. J. Beenakker, Spontaneous emission in chaotic cavities, Phys. Rev. Lett. **79**, 1841 (1997).

[48] Y. V. Fyodorov, D. V. Savin, and H.-J. Sommers, Parametric correlations of phase shifts and statistics of time delays in quantum chaotic scattering: Crossover between unitary and orthogonal symmetries, Phys. Rev. E **55**, R4857 (1997).

[49] Y. V. Fyodorov and Y. Alhassid, Photodissociation in quantum chaotic systems: Random-matrix theory of cross-section fluctuations, Phys. Rev. A **58**, R3375 (1998).

[50] B. A. van Tiggelen, P. Sebbah, M. Stoytchev, and A. Z. Genack, Delay-time statistics for diffuse waves, Phys. Rev. E **59**, 7166 (1999).

[51] P. W. Brouwer, K. M. Frahm, and C. W. J. Beenakker, Distribution of the quantum mechanical time-delay matrix for a chaotic cavity, Waves Random Media **9**, 91 (1999).

[52] D. V. Savin, Y. V. Fyodorov, and H.-J. Sommers, Reducing nonideal to ideal coupling in random matrix description of chaotic scattering: Application to the time-delay problem, Phys. Rev. E **63**, 035202(R) (2001).

[53] T. Kottos and U. Smilansky, Quantum graphs: A simple model for chaotic scattering, J. Phys. A **36**, 3501 (2003).

[54] F. Mezzadri and N. J. Simm, Tau-function theory of chaotic quantum transport with $\beta = 1, 2, 4$, Commun. Math. Phys. **324**, 465 (2013).

[55] C. Texier and S. N. Majumdar, Wigner time-delay distribution in chaotic cavities and freezing transition, Phys. Rev. Lett. **110**, 250602 (2013).

[56] M. Novaes, Statistics of time delay and scattering correlation functions in chaotic systems. I. Random matrix theory, J. Math. Phys. (N.Y.) **56**, 062110 (2015).

[57] F. D. Cunden, Statistical distribution of the Wigner-Smith time-delay matrix moments for chaotic cavities, Phys. Rev. E **91**, 060102(R) (2015).

[58] Y. Huang, C. Tian, V. A. Gopar, P. Fang, and A. Z. Genack, Invariance principle for wave propagation inside inhomogeneously disordered materials, Phys. Rev. Lett. **124**, 057401 (2020).

[59] C. Texier, Wigner time delay and related concepts: Application to transport in coherent conductors, Physica (Amsterdam) **82E**, 16 (2016).

[60] E. Pollak and W. H. Miller, New physical interpretation for time in scattering theory, Phys. Rev. Lett. **53**, 115 (1984).

[61] R. Landauer and T. Martin, Barrier interaction time in tunneling, Rev. Mod. Phys. **66**, 217 (1994).

[62] H. G. Winful, Tunneling time, the Hartman effect, and superluminality: A proposed resolution of an old paradox, Phys. Rep. **436**, 1 (2006).

[63] C. G. B. Garrett and D. E. McCumber, Propagation of a Gaussian light pulse through an anomalous dispersion medium, Phys. Rev. A **1**, 305 (1970).

[64] S. Chu and S. Wong, Linear pulse propagation in an absorbing medium, Phys. Rev. Lett. **48**, 738 (1982).

[65] R. W. Boyd and D. J. Gauthier, Slow and fast light, in *Progress in Optics*, edited by E. Wolf (Elsevier Science, New York, 2002).

[66] M. D. Stenner, D. J. Gauthier, and M. A. Neifeld, The speed of information in a 'fast-light' optical medium, Nature (London) **425**, 695 (2003).

[67] G. M. Gehring, A. Schweinsberg, C. Barsi, N. Kostinski, and R. W. Boyd, Observation of backward pulse propagation through a medium with a negative group velocity, Science **312**, 895 (2006).

[68] L. J. Wang, A. Kuzmich, and A. Dogariu, Gain-assisted superluminal light propagation, Nature (London) **406**, 277 (2000).

[69] U. Bortolozzo, S. Residori, and J. P. P. Huignard, Slow and fast light: Basic concepts and recent advancements based on nonlinear wave-mixing processes, Laser Photonics Rev. **4**, 483 (2010).

[70] D. Angulo, K. Thompson, V.-M. Nixon, A. Jiao, H. M. Wiseman, and A. M. Steinberg, Experimental evidence that a photon can spend a negative amount of time in an atom cloud, arXiv:2409.03680.

[71] M. Asano, K. Y. Bliokh, Y. P. Bliokh, A. G. Kofman, R. Ikuta, T. Yamamoto, Y. S. Kivshar, L. Yang, N. Imoto, Ş. K. Özdemir, and F. Nori, Anomalous time delays and quantum weak measurements in optical micro-resonators, Nat. Commun. **7**, 13488 (2016).

[72] Ph. Balcou and L. Dutriaux, Dual Optical tunneling times in frustrated total internal reflection, Phys. Rev. Lett. **78**, 851 (1997).

[73] H. Kogelnik and H. P. Weber, Rays, stored energy, and power flow in dielectric waveguides, J. Opt. Soc. Am. **64**, 174 (1974).

[74] C. C. Chan and T. Tamir, Angular shift of a Gaussian beam reflected near the Brewster angle, Opt. Lett. **10**, 378 (1985).

[75] M. Merano, A. Aiello, M. P. Van Exter, and J. P. Woerdman, Observing angular deviations in the specular reflection of a light beam, Nat. Photonics **3**, 337 (2009).

[76] K. Y. Bliokh and A. Aiello, Goos–Hänchen and Imbert–Fedorov beam shifts: An overview, J. Opt. **15**, 014001 (2013).

[77] Y. Aharonov, D. Z. Albert, and L. Vaidman, How the result of a measurement of a component of the spin of a spin-$1/2$ particle can turn out to be 100, Phys. Rev. Lett. **60**, 1351 (1988).

[78] A. M. Steinberg, How much time does a tunneling particle spend in the barrier region?, Phys. Rev. Lett. **74**, 2405 (1995).

[79] Y. Aharonov, N. Erez, and B. Reznik, Superluminal tunnelling times as weak values, J. Mod. Opt. **50**, 1139 (2003).

[80] D. R. Solli, C. F. McCormick, R. Y. Chiao, S. Popescu, and J. M. Hickmann, Fast light, slow light, and phase singularities: A connection to generalized weak values, Phys. Rev. Lett. **92**, 043601 (2004).

[81] N. Brunner, V. Scarani, M. Wegmüller, M. Legré, and N. Gisin, Direct measurement of superluminal group velocity and signal velocity in an optical fiber, Phys. Rev. Lett. **93**, 203902 (2004).

[82] N. Brunner and C. Simon, Measuring small longitudinal phase shifts: Weak measurements or standard interferometry?, Phys. Rev. Lett. **105**, 010405 (2010).

[83] H. Cao, A. Dogariu, and L. Wang, Negative group delay and pulse compression in superluminal pulse propagation, IEEE J. Sel. Top. Quantum Electron. **9**, 52 (2003).

[84] See Supplemental Material at http://link.aps.org/supplemental/10.1103/nnk7-xy4v for additional details. The Supplemental Material includes information on numerical simulations of the ring graph in the frequency and time domains, an examination of the extreme low transmission and large pulse bandwidth limits, additional analytical calculation details, plots of the experiment data over a wide frequency range, details on the time domain pulse measurements, details on potential sources of statistical and systematic error in the experiments, and further background information on complex time delay.

[85] D. Waltner and U. Smilansky, Scattering from a ring graph—a simple model for the study of resonances, Acta Phys. Pol. A **124**, 1087 (2013).

[86] D. Waltner and U. Smilansky, Transmission through a noisy network, J. Phys. A **47**, 355101 (2014).

[87] M. Białous, P. Dulian, A. Sawicki, and L. Sirko, Delay-time distribution in the scattering of short Gaussian pulses in microwave networks, Phys. Rev. E **104**, 024223 (2021).

[88] A. Akhshani, M. Białous, and L. Sirko, Quantum graphs and microwave networks as narrow-band filters for quantum and microwave devices, Phys. Rev. E **108**, 034219 (2023).

[89] P. Sebbah, O. Legrand, and A. Z. Genack, Fluctuations in photon local delay time and their relation to phase spectra in random media, Phys. Rev. E **59**, 2406 (1999).

[90] B. Macke and B. Ségard, Propagation of light-pulses at a negative group-velocity, Eur. Phys. J. D **23**, 125 (2003).

[91] M. A. I. Talukder, Y. Amagishi, and M. Tomita, Superluminal to subluminal transition in the pulse propagation in a resonantly absorbing medium, Phys. Rev. Lett. **86**, 3546 (2001).

[92] M. V. Berry and S. Popescu, Evolution of quantum superoscillations and optical superresolution without evanescent waves, J. Phys. A **39**, 6965 (2006).

[93] M. V. Berry, Optical currents, J. Opt. A **11**, 094001 (2009).

[94] N. Shaibe, J. M. Erb, and S. M. Anlage, Superuniversal statistics of complex time delays in non-Hermitian scattering systems, Phys. Rev. Lett. **134**, 147203 (2025).

[95] J. Erb, N. Shaibe, R. Calvo, D. P. Lathrop, T. M. Antonsen, T. Kottos, and S. M. Anlage, Topology and manipulation of scattering singularities in complex non-Hermitian systems: Two-channel case, Phys. Rev. Res. **7**, 023090 (2025).

[96] A. Giovannelli, Data used in imaginary time delay paper, http://hdl.handle.net/1903/33934.